A. Aertsen V. Braitenberg (Eds.)

Information Processing in the Cortex

Experiments and Theory

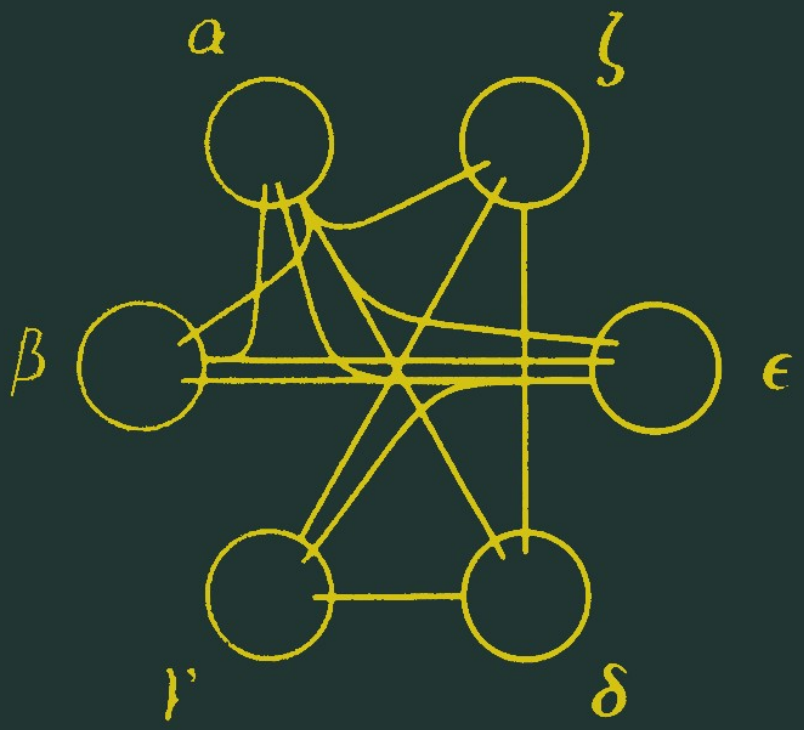

Springer-Verlag


ALLE ZEIT WACH
1842

Ad Aertsen Valentino Braitenberg (Eds.)

Information Processing in the Cortex

Experiments and Theory

With 102 Figures

Springer-Verlag
Berlin Heidelberg New York
London Paris Tokyo
Hong Kong Barcelona Budapest

Dr. Ad Aertsen
Universität Bochum
Institut für Neuroinformatik
Postfach 102148
Gebäude ND 04
W-4630 Bochum, FRG

Professor Dr. Valentino Braitenberg
Max-Planck-Institut
für biologische Kybernetik
Spemannstraße 38
W-7400 Tübingen, FRG

ISBN 978-3-642-49969-2 ISBN 978-3-642-49967-8 (eBook)
DOI 10.1007/978-3-642-49967-8

Library of Congress Cataloging-in-Publication Data.
Information processing in the cortex: experiments and theory / edited by Ad Aertsen and Valentino Braitenberg. p. cm. Includes bibliographical references and index.
ISBN 978-3-642-49969-2 (U.S.)
1. Cerebral cortex. 2. Human information processing. 3. Cognitive neuroscience. I. Aertsen, Ad (Adrianus), 1948–. II. Braitenberg, Valentino. QP383.I54 1992 612.8'25–dc20 92-19742 CIP

Typesetting: Camera ready by Margarete Ghasroldashti, MPI, Tübingen
31/3145-5 4 3 2 1 0 – Printed on acid-free paper

Current Source Density Analysis of Spatio-Temporal Fluorescence Maps in Organotypical Slice Cultures

Dietmar Plenz and Ad Aertsen[1]

Max-Planck-Institut für biologische Kybernetik, Spemannstrasse 38, 7400 Tübingen, Germany

Spatio-temporal spreading of activity in the CA3 region of organotypical slice cultures from the rat hippocampus was studied by measuring the intracellular potential distributions, using the optical recording technique. To enhance the spatial resolution, a specifically developed CSD-like transformation was applied to the fluorescence maps, enabling to calculate the locations of the transmembrane current generators (iCSD).

The iCSD-profiles provided a surprisingly good basis for the interpretation of spatio-temporal activity in the organotypical cultures, moreover, at a much higher spatial resolution than the original amplitude-latency fluorescence profiles. On the basis of these iCSD-profiles, the existence of aberrant projections between the CA1 and CA3 regions was revealed.

Introduction

Over the last years, organotypical slice cultures (Gähwiler 1989) gained considerable attention as a preparation to study the dynamics in nervous tissue under physiological, pharmacological and developmental considerations. Such quasi two-dimensional tissue preparations particularly provide a convenient possibility for studying the reorganization of intrinsic and/or the development of new fibre systems by mapping the spatio-temporal dynamics of the electrical activity. One of the

---

[1] present address: Institut für Neuroinformatik, Ruhr-Universität, P.O. Box 102 148, 4630 Bochum, Germany

methods to do this, the calculation of Current-Source Density profiles on the basis of the extracellular field potential distribution (*CSD*, Freeman and Nicholson 1975; Mitzdorf 1985), however, is particularly difficult in cultures. The main reason for this is the problem of assuring stable field potential measurements in such thin, quasi-monolayered tissue preparations.

Recently, another technique was developed to map the spatio-temporal dynamics of electrical activity in nervous tissue. This new technique of 'optical recording' consists of measuring the changes in optical properties of the tissue during neural activity (Grinvald et al. 1988; Salzberg 1989). Optical recording, particularly by application of voltage-sensitive fluorescent dyes to the nervous tissue, provides the opportunity to measure the summated intracellular activity of neuronal populations as well as the glia activity involved. It can be easily used to assess the spatio-temporal patterns of activity in *in vivo* (e.g. Grinvald et al. 1986) and *in vitro* (e.g. Bonhoeffer and Staiger 1988) preparations. The interpretation of these optical signals on the basis of their latency and amplitude distributions, however, does not achieve the spatial resolution obtained with classical CSD-analysis of field potential distributions from similar vertebrate tissue preparations.

In order to improve the spatial resolution and, hence, the interpretability of the fluorescence activity maps, we adopted the following approach. After rigorously identifying the fluorescence signals with the intracellular population activity integrated over a number of nerve cells or nerve cell circuits per unit tissue volume, we calculated from these signals the transmembrane current densities as viewed from the intracellular space (iCSD, Plenz and Aertsen 1991a,b). Thus, we combined the convenient method of optical recording with the high spatial resolution of the Current Source Density approach.

Here we used this newly developed transformation to study the various fibre projection areas in the CA3 region in organotypical slice cultures from the rat hippocampus.

Methods

Transverse organotypical hippocampal cultures from 4 to 7 days old rats were prepared by using the roller tube technique (Gähwiler 1989;

Caeser and Aertsen 1991). For recording, cultures were transferred to the recording chamber, which was mounted on an inverted microscope (Zeiss, IM35), equipped with an epifluorescence filter set (Zeiss, BP 546, FT 580, LP 590). The chamber was continuously perfused with HBSS (Gibco), to which were added 350 mg/l $NaHCO_3$ and 294 mg/l $CaCl_2x2H_20$. The latter was not added in case of calcium-free conditions. The flow rate was set to 0.5 ml/min and the temperature kept at 33.0 ± 0.1 °C. Slice cultures were lying submerged on thin coverslips. The voltage-sensitive styryl dye RH237 was applied to the bathing medium for 15 minutes before each experiment. Monopolar tungsten micro-electrodes were used for electrical double-pulse stimulation (ISI 40 ms) of the mossy fibres (first stimulus) and the alveus of the CA1 region (second stimulus).

For optical recording, cultures were illuminated by a mercury lamp (Zeiss, HWO 100 W/2, duration of trials 96 ms). The image of the nervous tissue was projected with an objective (Leitz, 25x NPL Fluotar, 0.75 oil immersion) onto a 12x12 photodiode array (Centronics, M144-5). The photodiode currents were amplified, multiplexed and fed into a microcomputer (DEC LSI 11/73) at a sample rate of 2 kHz per channel. The data were transferred to a VAX 750 (DEC) for further processing (Bonhoeffer and Staiger 1988). Each photodiode integrated the fluorescence over an area of 60x60 μm^2. In order to cover the entire depth of the CA3 region, a montage of two 12x12 fields with a spatial overlap of 33% was made, thus simulating an 20x12 photodiode array (cf. Fig. 2b). From the photodiode matrix a one-dimensional array of photodiodes was selected for the calculation of one-dimensional iCSD-profiles.

The fluorescence change dF was calculated for each separate location by taking the difference in fluorescence between successive trials with and without a stimulus (Procedure I; Bonhoeffer and Staiger 1988), or alternatively, as the difference between the response to a stimulus and a linear approximation of the non-stimulus sweep, based on the start and end points of the corresponding stimulus sweep (Procedure II). The relative fluorescence change dF/F was obtained by dividing this difference by the absolute fluorescence at that same location. Generally, we averaged the responses over 6 to 8 trials.

Under the assumptions of a quasi-static electric field and an extracellular space which behaves as an ohmic conductor with approximately constant conductivity, the CSD-profile is proportional to the second-order spatial derivative of the extracellular field potential dis-

tribution (eCSD). In addition, if the field potentials change predominantly along one-dimension only, the true eCSD-distribution can be approximated by applying the one-dimensional eCSD-analysis (Mitzdorf 1985) according to the formula:

$$-I_m(z,t) \sim \frac{U(z-n\Delta h,t) - 2U(z,t) + U(z+n\Delta h,t)}{(n\Delta h)^2} \qquad (1)$$

where $I_m(z,t)$ indicates the transmembrane current, U(z,t) is the field potential at position z and time t, Dh denotes the sampling interval between adjacent recording locations, and nDh is the differentiation grid size.

For the calculation of 1-dimensional CSD-profiles on the basis of relative fluorescence changes, we developed a very similar transformation (iCSD, Plenz and Aertsen 1991b). In short, we made the following main assumptions: (1) the orientation of the linear photodiode array is parallel to the main orientation of the recorded cells in the nervous tissue, (2) the distance between two photodiodes is much smaller than the extent of the activated cells seen by each photodiode, and (3) the intracellular space can be approximated by a purely ohmic resistance R_i. Then, for any point in time, the distribution of relative fluorescence change dF/F over the photodiode array is linearly related to the distribution of the intracellular membrane potential U_i along the dendrosomatic axis:

$$U_i(k,t) = K\,(dF/F)(k,t) \qquad (2)$$

with the proportionality constant K and compartment number k. The current i(k) in the intracellular space between two adjacent compartments k-1 and k, measured by the corresponding photodiodes, is described by

$$i(k) = KR_i^{-1}(k)\,\frac{(dF/F)(k) - (dF/F)(k+1)}{\Delta z} \qquad k \in [1,\ldots,m-1] \qquad (3)$$

where m represents the total number of compartments, and Dz is the width of a single compartment. From Equations (2) and (3), and

assuming (4) a constant intracellular resistance along the dendrosomatic axis, it follows that the current density $i_m(k)$ is proportional to the second spatial derivative of the fluorescence signal distribution:

$$I_{m(z,t)} \sim - \frac{(dF/F)_{(z-nDz,t)} - 2\,(dF/F)_{(z,t)} + (dF/F)_{(z+nDz,t)}}{(n\Delta z)^2} \qquad (4)$$

where z indicates the spatial dimension along the photodiode array and t denotes time. Finally, since sinks/sources in the intracellular space are seen as sources/sinks from the extracellular space, a sign inversion has to be made. The integer n was set equal to one. This then defines the transformation which was applied to the fluorescence distribution in order to calculate the iCSD-profiles. Notice the strong similarity between Equ. (4) and the classical one-dimensional CSD-analysis described by Equ. (1): the role of the extracellular field potential distribution U has simply been taken by the relative fluorescence distribution dF/F.

Results

A sketch of the recording situation is given in Fig. 1. The dashed frame indicates the area from which the optical recordings were made. Fig. 2a shows a photomontage of the CA3 region, with the pyramidal cell body layer clearly visible. The entire 20x12 matrix of photodiode responses, together with an indication of the anatomical borders, can be seen in Fig. 2b. Each trace in this plot represents the time course of the relative fluorescence change under high calcium condition, measured by a photodiode at the corresponding matrix location. From this matrix we selected the indicated row of photodiode responses for calculation of the iCSD-profile; this row was oriented in parallel to the main axis of the CA3 pyramidal cells.

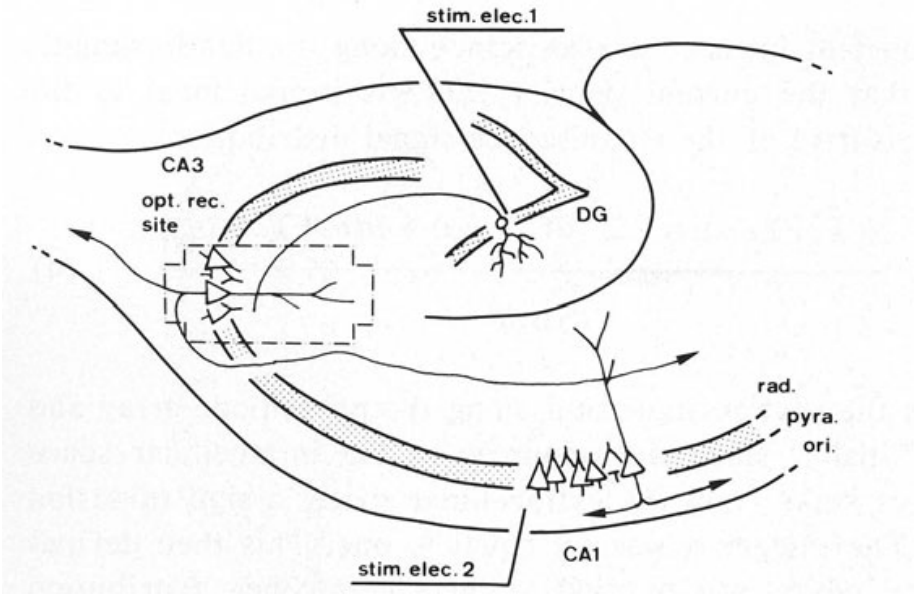

Fig. 1. Sketch of the anatomical and experimental situation in hippocampal organotypical slice cultures. *DG* gyrus dentatus; *rad.* stratum radiatum; *pyra.* stratum pyramidale; *ori.* stratum oriens; *stim.elec.1* stimulus electrode in the mossy fibres; *stim.elec.2* stimulus electrode in the alveus of the CA1 region; *opt.rec.site* location of photodiode matrix

Fluorescence maps and iCSD-profiles from the CA3 region of organotypical slice cultures

The following Figures 3 to 6 show typical results for the fluorescence maps and the calculated iCSD-profiles under different calcium levels. Negative deflections in the relative fluorescence changes, indicating intracellular depolarisations, are drawn upwards. In the iCSD-profiles, sinks are drawn upwards and sources downwards, as viewed from the extracellular space.

The fluorescence map under high calcium concentration (3.5 mM), calculated according to correction procedure I (see Methods), and the corresponding iCSD-profile are presented in Fig. 3. In the fluorescence map (Fig. 3a) we observe that a few milliseconds after the stimulus in the mossy fibres (i.e. the first stimulus), depolarisations occur in the entire CA3 region. The shortlasting peak at the beginning of the depolarization in the stratum pyramidale indicates the presence of action potentials (* in Fig. 3a). The response to stimulation of the alveus (second stimulus) looks nearly the same as the response to the mossy fiber stimulus, the only difference being that the initial peak in the stratum pyramidale is missing.

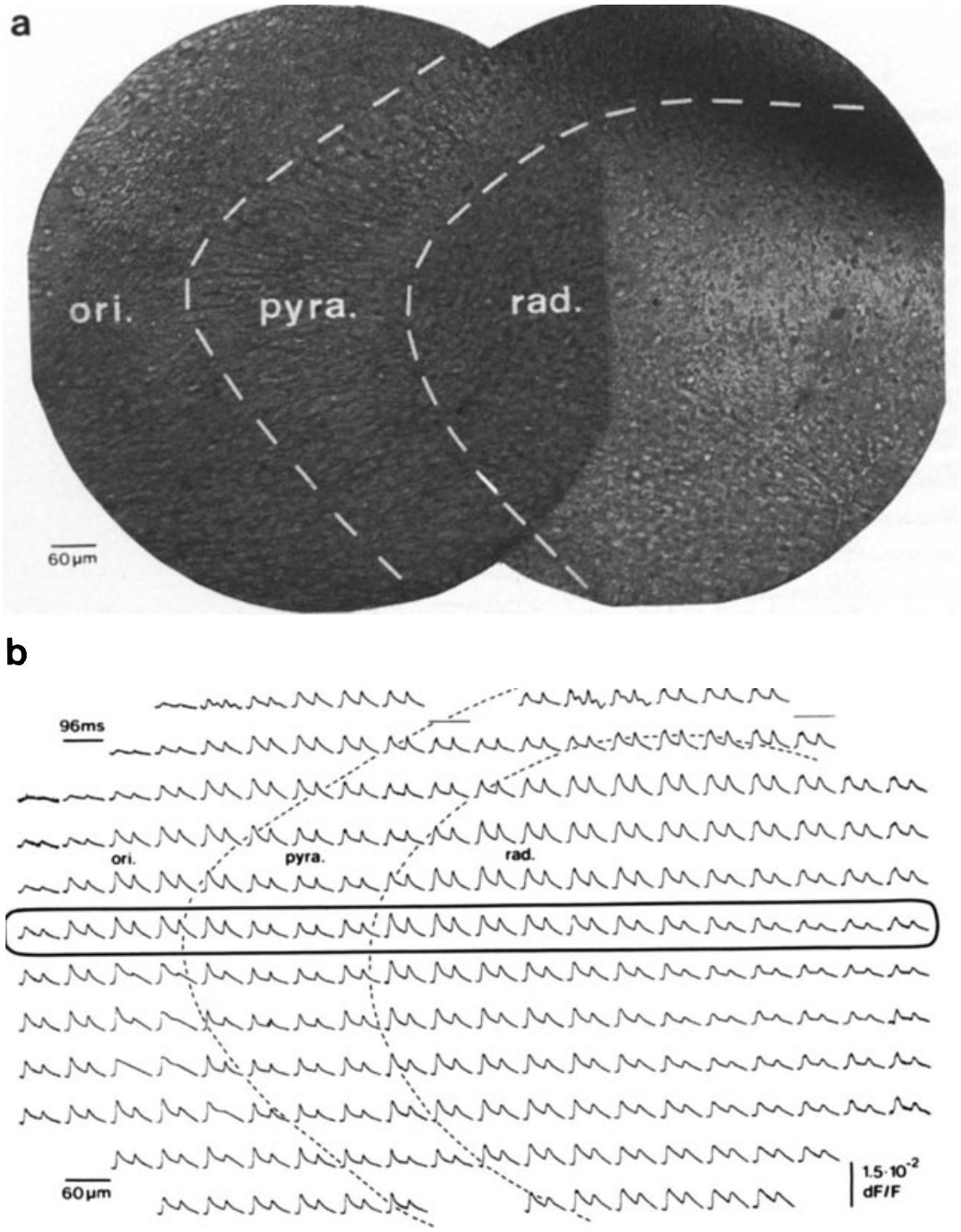

Fig. 2. Optical recording from the CA3 region of organotypical hippocampal slice cultures. **a**: Photographic view of the CA3 area, monitored by the optical recording; **b**: Optical recording of the activity in the CA3 region under high calcium conditions (3.5 mM). Each trace (duration 96 ms) displays the averaged activity (6 stimuli) recorded by a single photodiode from the corresponding tissue location. The encircled row of photodiodes was selected for calculation of the iCSD-profile (Fig. 3). *rad.* stratum radiatum; *pyra.* stratum pyramidale; *ori.* stratum oriens

From anatomical considerations on organotypical hippocampal cultures (Zimmer and Gähwiler 1984; Caeser and Aertsen 1991), we propose

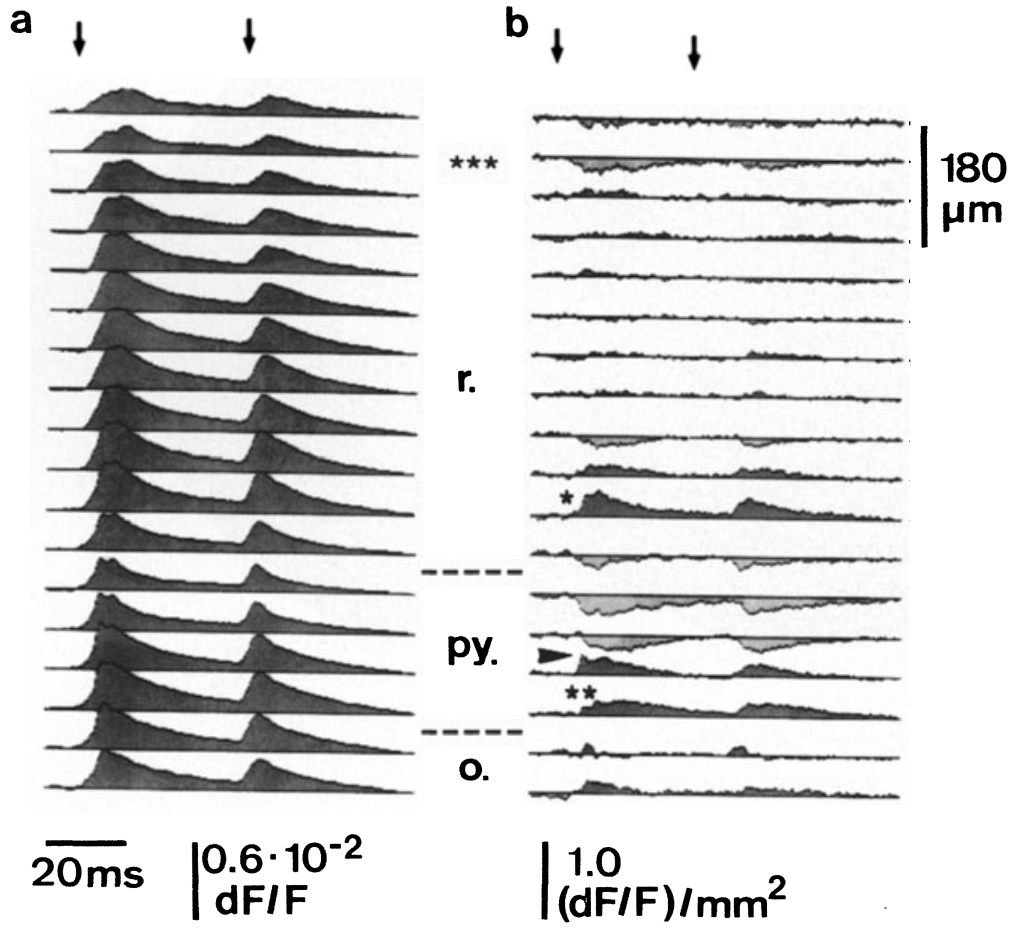

Fig. 3. Distribution of relative fluorescence change (**a**) under high calcium conditions (3.5 mM; encircled row of fluorescence signals in Fig 2b) and associated iCSD-profile (**b**). In this case correction procedure I (Methods) was applied to determine the relative fluorescence change

that the response to the first stimulus is mainly due to synaptic activation by the mossy fibres, resulting in spike activity in the CA3 pyramidal cells. It is well known, however, that the anatomical termination area of mossy fibres on CA3 pyramidal cells is on the proximal dendritic tree. Consequently, one would expect the synaptic depolarisations to arise mainly in the vicinity of the pyramidale/radiatum border, rather than being distributed over the whole stratum radiatum (comp. Figs. 2a,b and 3a). At least two reasons may account for this discrepancy: either the course of the mossy fibre bundle is less well preserved in hippocampal slice cultures, or the location of the synaptic input cannot be judged with enough precision from the relative fluorescence maps.

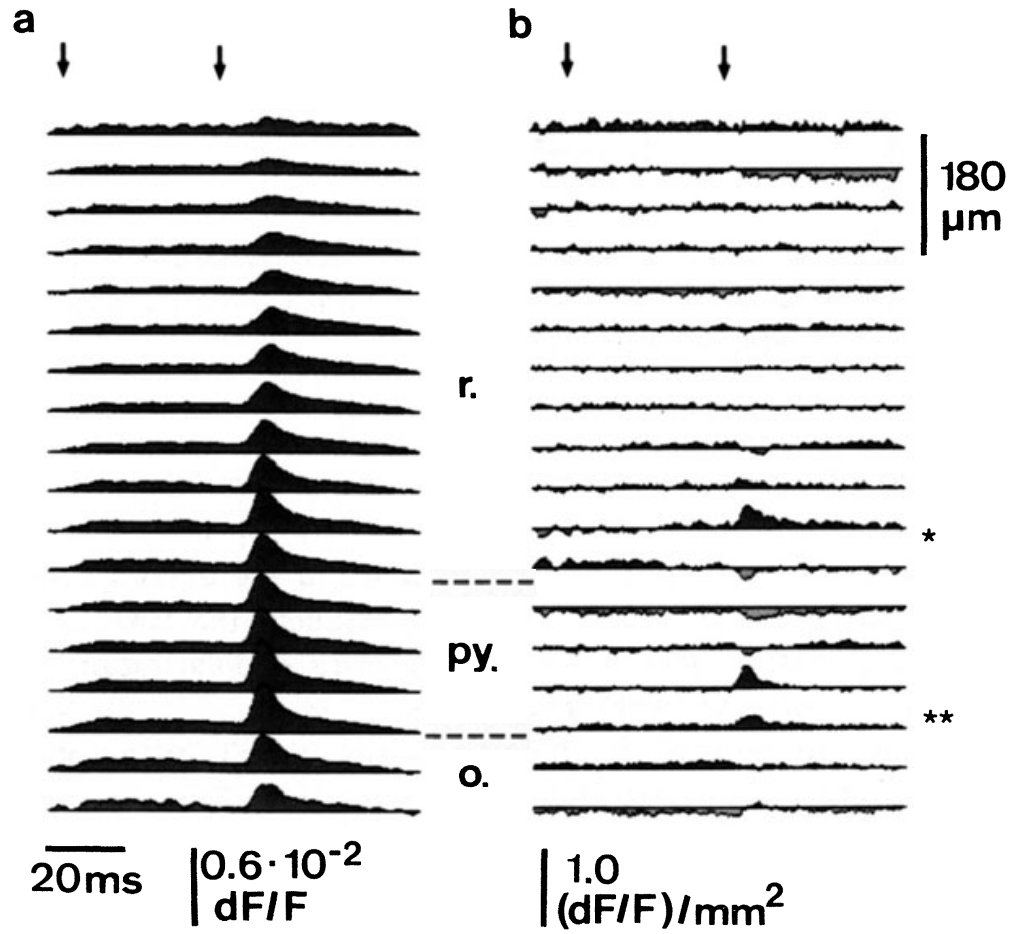

Fig. 4. Distribution of relative fluorescence change (**a**) unter high calcium conditions (3.5 mM) and associated iCSD-profiles (**b**) of the same experimental data as in Fig. 3. In this as well as in all following cases correction procedure II (Methods) was applied

Similarly, for the response to stimulation of the alveus one would expect mainly antidromically induced spike activity in the stratum pyramidale, together with synaptic or spike activity in the outer region of stratum pyramidale due to axonal collaterals. Hence, the two large depolarisation areas, particularly the large and early depolarisation in the stratum radiatum, are somewhat unexpected.

Faced with these differences, it would be highly beneficial to apply a transformation, which increases the spatial resolution. This can indeed be achieved, as witnessed by the iCSD-profiles shown in Figs. 3b and 4b. In these plots, sinks (i.e. positive ions flowing into the cell) are indicated as upwards deflections and, likewise, sources as downward deflections. Hence, areas which mark excitatory synaptic influx show up as sinks with a monophasic time course, joined by similar adjacent

sources. Using this criterion, the analysis of the responses to both the mossy fibre stimulus and the alveus stimulus, reveals two synaptic input areas (* and ** in Figs. 3b and 4b). In addition, however, the iCSD-profile in Fig. 3b shows longlasting, negative and positive ramps at a number of locations. We presume that these longlasting events in the iCSD-profiles are artefacts, due to an incorrect normalization for bleaching and inhomogeneities in the fluorescence plots, and amplified by the CSD-analysis. As an alternative, therefore, we used procedure II (see Methods). The results from the same experimental data are shown in Fig. 4. The differences achieved in the fluorescence maps can be recognized by comparing Figs. 3a and 4a: the overall depolarization in the fluorescence distribution is strongly diminished. As a result, the associated iCSD-profile (Fig. 4b) shows a much clearer distribution of sinks and sources. We will use this correction procedure II for all profiles to follow. The adequacy of this correction will be elaborated in the Discussion.

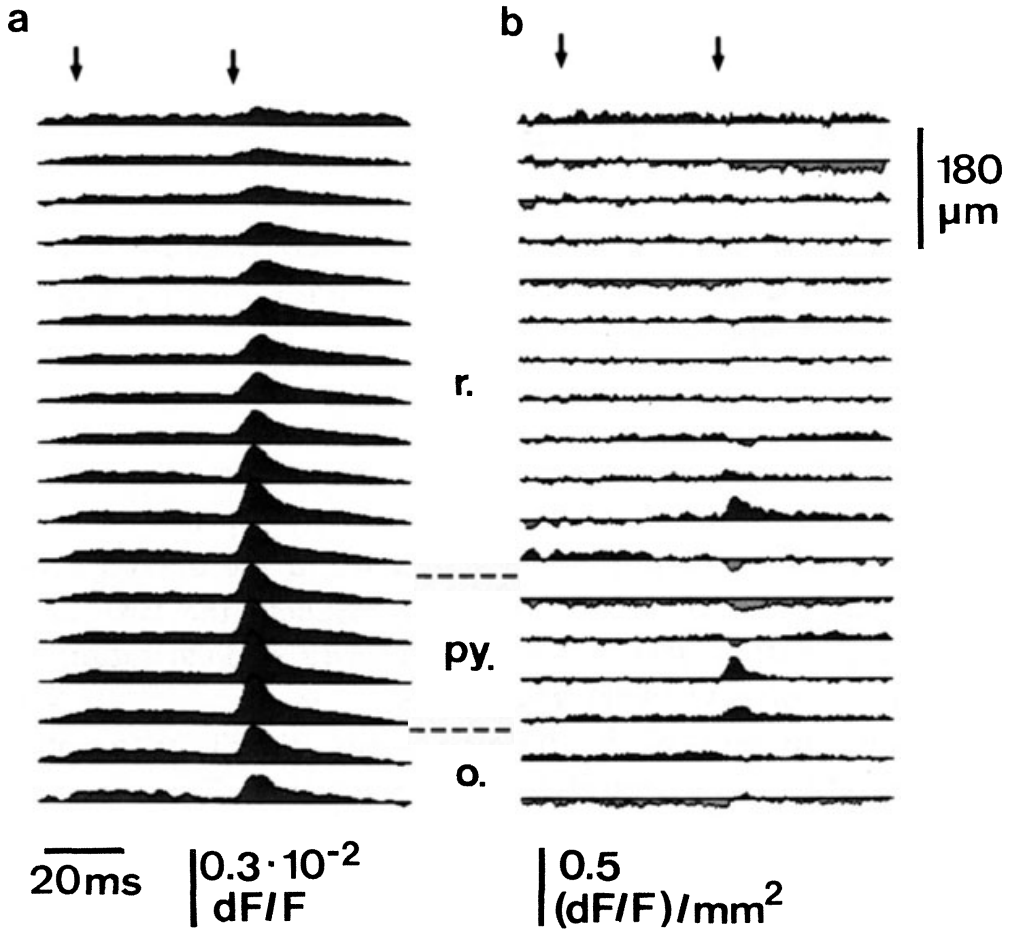

Fig. 5. (a) Relative fluorescence change unter calcium-free conditions; (b) associated iCSD-profile.

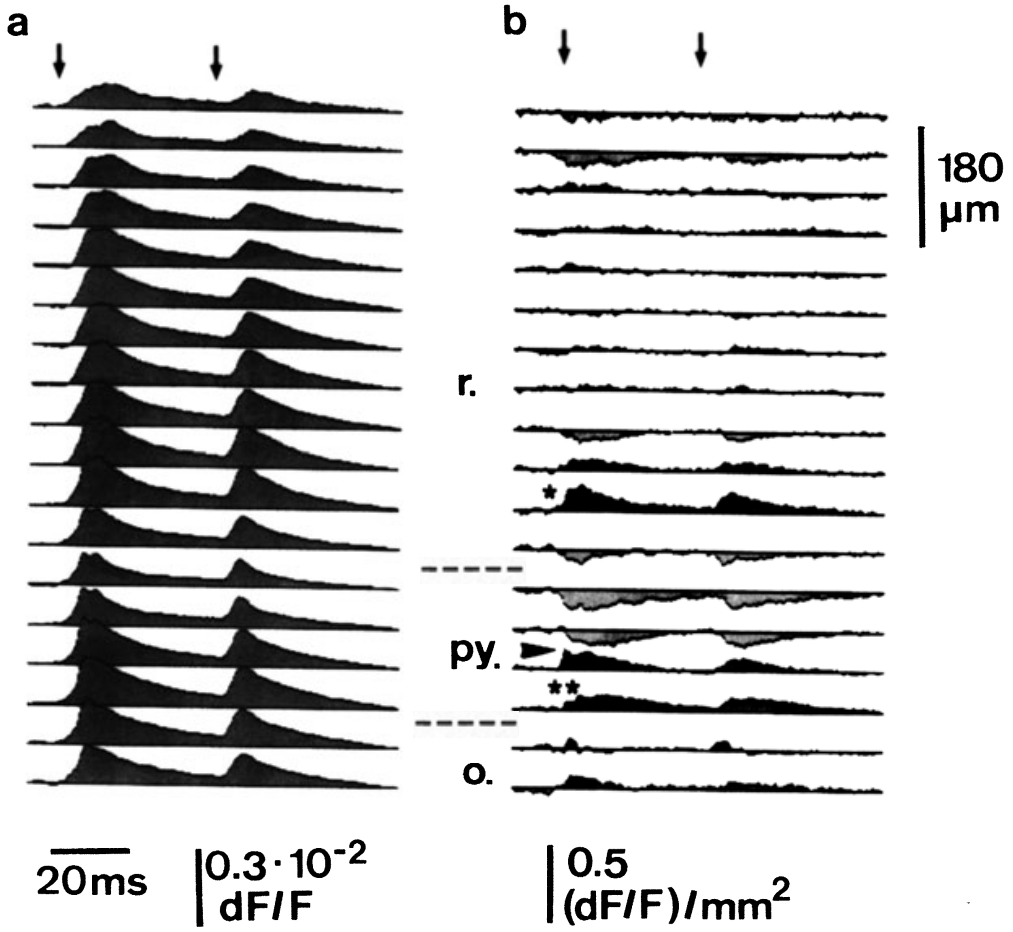

Fig. 6. Recovery of responses 30 min after the change from calcium-free to high calcium conditions. Distribution of relative fluorescence change (**a**) and associated iCSD-profile (**b**)

The first response in the iCSD-profile in Fig. 4b shows a clear sink with adjacent sources in the stratum radiatum and stratum pyramidale (*). This sink is now situated close to the pyramidale/radiatum border, as was expected from the mossy fiber termination area. A second sink, appearing in the outer region of the stratum pyramidale (**), indicates the presence of additional synaptic input. This latter feature occurs in both responses. Additional sinks show up in the distal dendritic region (***). These reflect activity in the dendate gyrus. Finally, the small action potential pattern in the stratum pyramidale (arrowhead) will be shown and discussed in greater detail later (cf. Fig. 7a).

In order to separate synaptically and antidromically evoked responses, we performed the same experiment under calcium-free conditions. The results are shown in Fig. 5. In this case, the fluorescence map and the iCSD-profile only reveal responses to stimulation of the alveus.

The iCSD-profile (Fig. 5b) shows the composite sink/source profile of antidromically generated action potentials in the stratum pyramidale. The adjacent sinks above and below reflect both passive compensation and active propagation (Plenz and Aertsen 1991b). Thirty minutes after changing the calcium-free medium to high calcium again, the response recovered, albeit incompletely with respect to the first stimulus (Fig. 6b). Again, the response to stimulation of the alveus reveals two distinct sinks. At the location marked with (*) we now also discern an additional, biphasic sink/source time course, superimposed on the monophasic sink. This feature is considered in more detail in Fig. 7.

The iCSD-profiles in the stratum pyramidale under high calcium conditions, already shown in Figs. 4b and 6b, are replotted at higher magnification in Fig. 7. Consider first the response before calcium-free conditions were imposed (Fig. 7a). In the response to the mossy fibre stimulation (first stimulus) we discern a biphasic sink/source

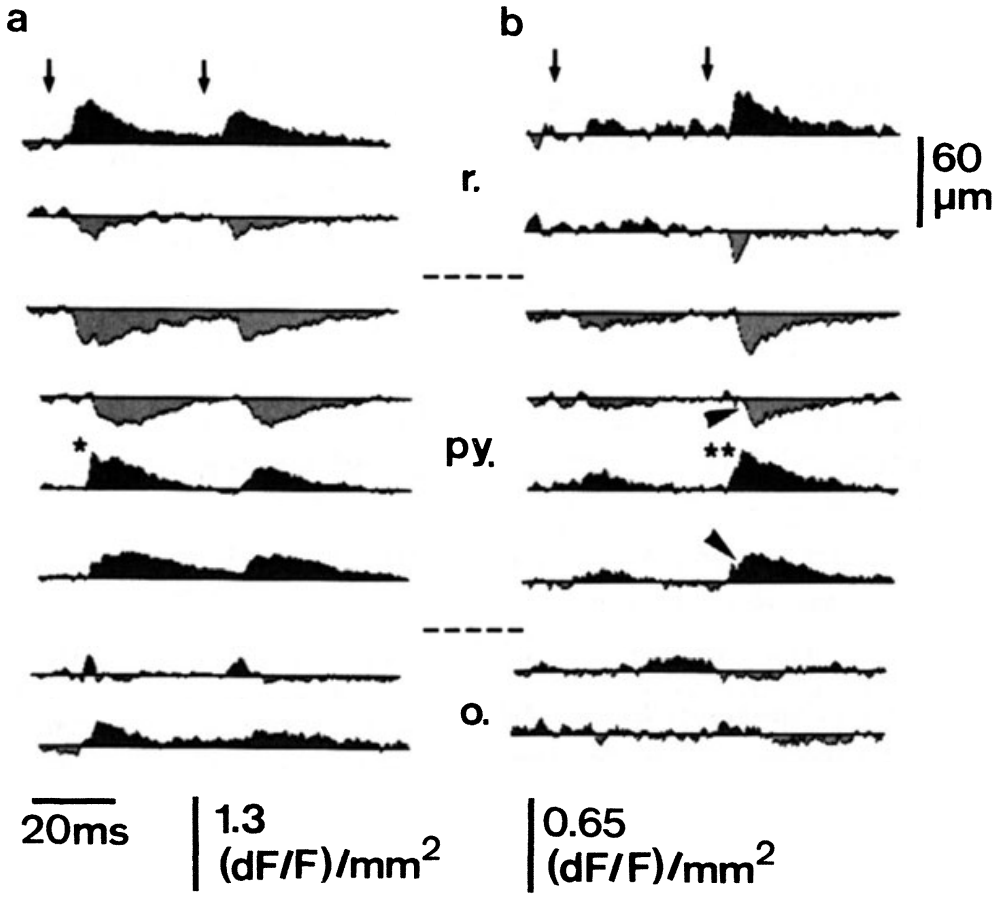

Fig. 7. Enlarged view of the iCSD-profiles in the stratum pyramidale from Fig. 3b (**a**) and Fig 5b (**b**)

waveform, superimposed on a sink (*). Such a biphasic waveform does not arise in the response to stimulation via the alveus (second stimulus), indicating that no pyramidal cell body action potentials arise in this case. The latter can be explained by the phenomenon of double-pulse inhibition. In contrast to this, Fig. 7b shows that under the condition of partial recovery from calcium-free medium, when mossy fiber stimulation failed to elicit action potentials in the pyramidal cell body layer, stimulation in the alveus does succeed to evoke action potentials. This is indicated by the sharp sink riding on the basal sink (**), the corresponding short-lasting source in the lower trace (arrowhead) and the steepening of the source in the upper trace (arrowhead).

Discussion

The purpose of the present study was to investigate the flow of neural activity in area CA3 of organotypical slice cultures of the rat hippocampus. In particular, we focussed on the question of orderly development of fibre bundle projections in such slice cultures. We approached these issues by studying CSD-profiles obtained from relative fluorescence maps (iCSD). Before turning to the results, we will first discuss a number of methodological aspects of the optical recording technique.

Methodological aspects of fluorescence maps in organotypical slice cultures

In general, it is nearly impossible to determine the precise origin of the fluorescence signal, collected by a single photodetector (Grinvald et al. 1988). However, in the organotypical hippocampal slice culture, because of its orderly topography, we made the assumption that each photodiode is collecting the activity from a tissue area which is dominated by a particular type of cell elements: we measure mainly dendritic activity in the stratum radiatum, cell body activity in the stratum pyramidale, and axonal. activity in the stratum oriens/alveus region.

We used two different procedures to calculate the relative fluorescence dF/F. From theoretical considerations, subtraction of the non-stimulus sweep from the stimulus sweep (procedure I) should be the

most adequate approach. In our experiments we observed, however, that the light source may undergo slow, but considerable amplitude changes from trial to trial. Clearly this leads to residual terms when subtracting successive stimulus and non-stimulus sweeps. Although these residues tend to cancel when averaging over many trials, they give rise to distinct artefacts when working with low numbers of stimuli, as demonstrated by the long-lasting positive or negative dilatations in the iCSD-profile in Fig. 3b. The spurious nature of these features is underlined by the lack of correlation with location within the tissue when comparing across experiments. As a simple alternative, we chose to apply correction procedure II, which uses a linear approximation of the non-stimulus sweep and, thus, avoids the nonstationarity problem altogether.

CSD-profiles of relative fluorescence distributions (iCSD)

Several assumptions had to be made in the calculation of the iCSD-profile (see Methods and extensive discussion in Plenz and Aertsen 1991b). For the orderly arranged CA3 pyramidal cells in organotypical hippocampal slice cultures, the first assumption is fulfilled by properly orienting the photodiode array in parallel to the cells' main axis (Fig. 2a,b). Assumption (2), high spatial resolution, is implicit in the reasoning on different cell compartments. In addition, the required distance between neighboring photodiodes should be based upon a spatial Fourier analysis of the fluorescence distribution (Plenz and Aertsen 1991b). Assumption (3) stating that the intracellular resistance can be considered as purely ohmic, is based on the ionic nature of the intracellular medium.

Finally, some special attention should be given to assumption (4): constant intracellular resistance along the dendrosomatic axis. This assumption clearly contradicts the observation that this resistance is, amongst others, a function of the diameter of the different cell compartments, and is regarded to be highest in the axonal branches and lowest in the cell body region. Consequently, this assumption introduces a systematic error in the iCSD-profiles, calculated on the basis of Equ. (4): the cell body region compartments receive less weight than the dendritic and axonal compartments. As a result, iCSD-profiles preferentially reveal their activity in the strata radiatum and oriens, at

the expense of activity in the stratum pyramidale (for a discussion on additional procedures we refer to Plenz and Aertsen 1991b).

Abberrant projections in the organotypical slice culture of rat hippocampus

We found that any attempt to unravel the underlying processes in the CA3 region on the basis of amplitude-latency distributions of the fluorescence maps is seriously hampered by the lack of adequate spatial resolution. This refers to the problem of determining the location of synaptic input as well as the differentiation between active and passive events. In this respect, the introduction of iCSD-profiles presents a significant improvement when interpreting the spatio-temporal activity patterns. For instance, the position of the synaptic sink in the stratum radiatum matches the location one would expect from the neuroanatomy.

In addition, it could be shown that the activity in the stratum pyramidale and in the border region of stratum pyramidale and stratum oriens consists of a mixture of action potentials and a second synaptic sink. The slight time delay between the first and second sink suggests that the latter is due to the activation of inhibitory interneurons via recurrent axon collaterals from the CA3 pyramidal cells (Schwartzkroin and Knowles 1983). This interpretation of recurrent inhibition is in accordance with the finding that an action potential pattern is lacking in the response to the second stimulus, if action potentials were elicited in the first response (Fig. 4b). Such double-pulse inhibition has, in fact, been observed in organotypical cell cultures (Cornish and Wheal 1989; Caeser et al. 1990), and is to be expected because of the presence of GABAergic neurons in such cultures (Caeser and Aertsen 1991). The synaptic sink in the stratum oriens of the CA3 region, however, could also result from sprouting of the mossy fibres. This phenomenon was reported for kindled rats (Ben-Ar and Represa 1990) and could therefore also be expected in cultures, which are known to have a tendency for epileptic behaviour (Furshpan and Potter 1989; Koroshetz and Furshpan 1990).

The presence of antidromically evoked action potentials in the iCSD-profiles under calcium-free conditions clearly reveals the presence of abberant axonal projections in organotypical hippocampal slice cultures. In the case of alveus stimulation under high calcium conditions, this AP-pattern is lacking and, instead, a synaptic sink shows up

in the stratum radiatum and a second one in the stratum oriens (Fig. 4b). Whereas the former sink can again be attributed to the activation of inhibitory interneurons, two explanations may account for the second sink. It could either result from (not *in vivo* occurring) axonal projections of CA1 pyramidal cells into the CA3 region (Caeser and Aertsen 1991) or, alternatively, from aberrant projections of the Schaffer collaterals and their profound recurrent axon collaterals (Miles and Wong 1986; Ben-Ari and Represa 1990; Caeser and Aertsen 1991). The former possibility of an unusual target projection of the CA1 region in organotypical slice cultures is supported by findings of Zimmer and Gähwiler (1984) of an increased autoinnervation of the CA1 region.

Acknowledgements

We thank Volker Staiger for skillful assistance throughout the experiments and in the preparation of the Figures. In addition, we thank Ulla Mitzdorf for helpful discussions during the early stages of this work. Partial funding for this study was received from the Bundesministerium für Forschung und Technologie (BMFT).

References

Ben-Ari Y, Represa A (1990) Brief seizure episodes induce long-term potentiation and mossy fibre sprouting in the hippocampus. TINS 13:312-318

Bonhoeffer T, Staiger V (1988) Optical recording with single cell resolution from monolayered slice cultures of rat hippocampus. Neurosci Lett 92:259-264

Caeser M, Aertsen A (1991) Morphological organization of rat hippocampal slice cultures. J Comp Neurol 307:87-106

Caeser M, Plenz D, Aertsen A (1990) Spatio-temporal spreading of electrical activity in rat hippocampus slices and cell cultures. In: Elsner N, Roth G (eds) Brain - Perception - Cognition. Georg Thieme Verlag, Stuttgart New York

Cornish SM, Wheal HV (1989) Long-term loss of paired pulse inhibition in the kainic acid lesioned hippocampus of the rat. Neurosci 28:563-571

Freeman JA, Nicholson C (1975) Experimental organisation of current source density technique for anuran cerebellum. J Neurophysiol 38:369-382

Furshpan EJ, Potter DD (1989) Seizure-like activity and cellular damage in rat hippocampal neurons in cell culture. Neuron 3:199-207

Gähwiler BH (1989) Organotypic cultures of neural tissue. TINS 11:484-489

Grinvald A, Frostig RD, Lieke E, Hildesheim R (1988) Optical imaging of neuronal activity. Physiol Rev 68:1285-1366

Grinvald A, Lieke E, Frostig RD, Gilbert CD, Wiesel TN (1986) Functional architecture of cortex revealed by optical imaging of intrinsic signals. Nature 324:361-364

Koroshetz WJ, Furshpan EJ (1990) Seizure-like activity and glutamate receptors in hippocampal neurons in culture. Neurosci Res 8 Suppl. 13:S65-S74

Miles R, Wong RKS (1986) Excitatory synaptic interactions between CA3 Neurones in the Guinea-pig hippocampus. J Physiol (Lond) 373:397-418

Mitzdorf U (1985) Current source density method and application in cat cerebral cortex: Investigation of evoked potentials and EEG phenomena. Physiol Rev 65:37-100

Plenz D, Aertsen A (1991a) On the correspondance of intra- and extracellullar space: Convergence of classical field potential measurements and optical recording with voltage-sensitive dyes at the level of current source density analysis. In: Penzlin H, Elsner N (eds) Synapse - Transmission - Modulation. Thieme Verlag, Stuttgart, p 312

Plenz D, Aertsen A (1991b) Current Source Density profiles of optical recording maps: a new approach to the analysis of spatio-temporal neural activity patterns. (submitted)

Salzberg BM (1989) Optical recording of voltage changes in nerve terminals and in fine neuronal processes. Ann Rev Physiol 51:507-526

Schwartzkroin PA, Knowles WD (1983) Local interaction in the hippocampus. TINS 3:88-92

Zimmer J, Gähwiler BH (1984) Cellular and connective organization of slice cultures of the rat hippocampus and fascia dentata. J Comp Neurol 228:432-446